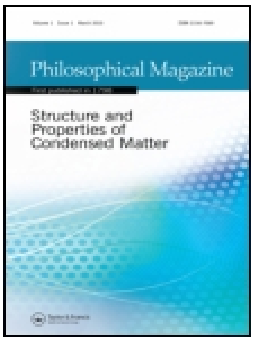

Philosophical Magazine

ISSN: 0031-8086 (Print) (Online) Journal homepage: http://www.tandfonline.com/loi/tphm19

The magnetic structure and hyperfine field of $FeGe_2$

J. B. Forsyth , C. E. Johnson & P. J. Brown

To cite this article: J. B. Forsyth , C. E. Johnson & P. J. Brown (1964) The magnetic structure and hyperfine field of $FeGe_2$, Philosophical Magazine, 10:106, 713-721, DOI: 10.1080/14786436408228489

To link to this article: http://dx.doi.org/10.1080/14786436408228489

The Magnetic Structure and Hyperfine Field of $FeGe_2$

By J. B. FORSYTH and C. E. JOHNSON
Solid State Physics Division, Harwell, Didcot, Berks.

and P. J. BROWN
Cavendish Laboratory, Cambridge

[Received 31 July 1964]

ABSTRACT

The magnetic structure of the intermetallic compound $FeGe_2$ has been determined from powder and single crystal neutron diffraction data. The unit cell of the anti-ferromagnetic array is the same size as the chemical cell, and the spins on the four equivalent iron atoms in this cell lie parallel or anti-parallel to two different, but symmetry related, directions in the basal plane of the tetragonal structure. The angle between the two spin directions is $71° \pm 6°$ and the moment per iron atom observed is $0{\cdot}73 \pm 0{\cdot}06\ \mu_B$. The temperature dependence of the magnetic scattering indicates a Néel point in the region of 0°C. The hyperfine field at the iron atom as determined from the Mössbauer effect is 148 ± 2 kG.

§ 1. INTRODUCTION

THE magnetic properties of the intermetallic compound $FeGe_2$ were first studied by Yasukochi *et al.* (1961); they observed the onset of weak ferromagnetism at 190°K and estimated the saturation magnetization at 0°K to correspond to $0{\cdot}11\mu_B$ per iron atom. A plot of the inverse susceptibility versus temperature indicated an effective Bohr magneton number of 2·43. They suggested that the parasitic ferromagnetism was due to vacant sites in the crystal lattice of an anti-ferromagnetic array and they proposed a spin scheme for the anti-ferromagnetic structure.

In the light of these observations we undertook an investigation of the magnetic structure of $FeGe_2$. Subsequently Airoldi and Pauthenet (1964) reported that they were unable to observe weak ferromagnetism in $FeGe_2$ for fields up to 20 koe in the temperature range 2–950°K. At temperatures between 500 and 950°K they observe a Curie–Weiss dependence of the susceptibility which indicates a magnetic moment of $2{\cdot}1\ \mu_B$ per iron atom. Our samples of $FeGe_2$ also failed to exhibit parasitic ferromagnetism at liquid nitrogen temperatures. It therefore seems likely that the ferromagnetism observed by Yasukochi *et al.* resulted from contamination of their specimens by the ferromagnetic compound Fe_5Ge_3.

§ 2. MATERIAL

Polycrystalline specimens of $FeGe_2$ were prepared by melting together the calculated quantities of iron wire and germanium lump at 1000°C under one-half an atmosphere of oxygen-free argon. The materials were spectrographically standardized and of better than 99·99% purity. The constitution of the polycrystalline material was checked using x-ray diffraction techniques and was found to have the tetragonal unit cell given by Wallbaum (1943) for $FeGe_2$.

A single crystal rod $20 \times 1 \times 1{\cdot}5$ cm of approximately elliptical section was grown for us by Mr. J. H. Harrison from the polycrystalline material. The crystal was grown under argon in an alumina boat using a travelling zone technique. The molten zone was moved through the crystal at 0·4 cm/hour. The axis of the crystal rod was found to be close to the normal to (111).

§ 3. DETERMINATION OF THE MAGNETIC STRUCTURE

Wallbaum (1943) has shown that $FeGe_2$ has the C16 ($CuAl_2$) structure. The space group of this structure is I4/mcm; the germanium atoms occupy the positions

$$\pm(x, \tfrac{1}{2}+x, 0) \qquad \pm(\tfrac{1}{2}+x, \bar{x}, 0)$$
$$\pm(\tfrac{1}{2}+x, x, \tfrac{1}{2}) \qquad \pm(x, \tfrac{1}{2}-x, \tfrac{1}{2})$$

and the iron atoms those at

$$\pm(0, 0, \tfrac{1}{4}) \qquad \pm(\tfrac{1}{2}, \tfrac{1}{2}, \tfrac{1}{4}).$$

Non-magnetic neutron reflections (hkl) can occur from this structure only if $h+k+l$ is even and in addition if either h or k is zero l must be even.

A single crystal pillar $2 \times 2 \times 8$ mm elongated parallel to [100] was cut from the crystal rod and used to measure the intensities of the ($0kl$) neutron reflections. At room temperature, reflections with either k or l odd were shown to be absent. At 100°K, however, additional intensity was measured in the positions of those reflections for which both k and l are odd and those for which k is odd and l is even. No reflections occurred with k even and l odd. In addition no reflections were observed which would indicate that the magnetic unit cell differed in size from the chemical one.

The positions of the iron atoms in the unit cell correspond, apart from a shift of origin, to those of the magnetic ions in $CrVO_4$, so that the conditions governing magnetic reflections in this structure which were derived by Frazer and Brown (1962) can be applied directly. If $\mathbf{S}_1$, $\mathbf{S}_2$, $\mathbf{S}_3$ and $\mathbf{S}_4$ are vectors giving the magnitude and direction of the spins on the iron atoms at $(0,0,\tfrac{1}{4})$, $(0,0,\tfrac{3}{4})$, $(\tfrac{1}{2},\tfrac{1}{2},\tfrac{1}{4})$ and $(\tfrac{1}{2},\tfrac{1}{2},\tfrac{3}{4})$ respectively, then we have the conditions

$$\mathbf{S}_1+\mathbf{S}_2+\mathbf{S}_3+\mathbf{S}_4=0$$

if there is no net moment, and

$$S_1^2=S_2^2=S_3^2=S_4^2,$$

since the four atoms are chemically identical. Under these conditions three orthogonal vectors $\mathbf{L}_1$, $\mathbf{L}_2$, $\mathbf{L}_3$ can be defined such that

$$\mathbf{L}_1=\mathbf{S}_1-\mathbf{S}_2-\mathbf{S}_3+\mathbf{S}_4,$$
$$\mathbf{L}_2=\mathbf{S}_1-\mathbf{S}_2+\mathbf{S}_3-\mathbf{S}_4,$$
$$\mathbf{L}_3=\mathbf{S}_1+\mathbf{S}_2-\mathbf{S}_3-\mathbf{S}_4.$$

Then, writing the structure factor for magnetic scattering in the form adopted by Frazer and Brown (1962)

$$F(hkl)=\sum_{j=1}^{j=4}[\mathbf{e}(\mathbf{e}\,.\,\mathbf{S}_j)-\mathbf{S}_j]\exp 2\pi i\,(hx_j+ky_j+lz_j)$$

as

$$F(hkl)=4[\mathbf{e}(\mathbf{e}\,.\,\mathbf{L}_k)-\mathbf{L}_k] \text{ with respect to an origin at } (0, 0, \tfrac{1}{4}),$$

where

$k=1$ for reflections with $h+k$ odd l odd,
$k=2$ for reflections with $h+k$ even l odd,
$k=3$ for reflections with $h+k$ odd l even,

and $\mathbf{e}$ is the scattering vector, the magnetic reflections observed indicate that $\mathbf{L}_1$ and $\mathbf{L}_3$ are finite and $\mathbf{L}_2=0$.

The integrated intensities of all magnetic reflections in the [100] zone out to $\sin\theta/\lambda=0{\cdot}32$ were measured. Using these measurements and assuming the form factor for iron measured by Pickart and Nathans (1961) least squares analyses were carried out to determine the components of the vectors L_1 and L_3 parallel and perpendicular to the c axis. The values derived were:

$$\left.\begin{array}{ll} L_{1xy}=2{\cdot}19\,\mu\text{B}, & L_{1z}=0{\cdot}68\,\mu\text{B}, \\ L_{3xy}=1{\cdot}52\,\mu\text{B}, & L_{3z}=0{\cdot}59\,\mu\text{B}. \end{array}\right\} \quad . \; . \; . \; . \; . \; . \quad (a)$$

In both cases the component parallel to z is small and since the scatter in the measurements is considerable this component is probably not significant. When the values of the xy components are re-calculated with the z component zero the values obtained are:

$$\left.\begin{array}{l} L_1=2{\cdot}38\pm0{\cdot}20\,\mu\text{B}, \\ L_3=1{\cdot}69\pm0{\cdot}08\,\mu\text{B}. \end{array}\right\} \quad . \; . \; . \; . \; . \; . \; . \; . \; . \quad (b)$$

The observed and calculated values for the magnetic scattering cross sections for the two models (a) and (b) is shown in table 1. It would appear that significantly better agreement is not obtained using the z components of the L vectors and we therefore prefer the model in which the spins are confined to the basal plane.

In all the calculations we have assumed a random distribution of tetragonally equivalent domains and this precludes determination of the orientation of either $\mathbf{L}_1$ or $\mathbf{L}_3$ within the basal plane; they must, however, by definition be orthogonal to one another.

The magnetic intensities were placed on an absolute scale by comparison with the nuclear intensities. Measurements made on the single crystal and those obtained from the power diffraction patterns were combined to establish the degree of extinction in the single crystal. To obtain the best fit with the nuclear intensities a value of $x=0{\cdot}155$ was derived for the parameter of the germanium atoms. The observed and calculated nuclear intensities are compared in table 2. The more intense reflections were found to suffer heavily from extinction. The powder neutron diffraction patterns obtained at room temperature and at 4·2°K are reproduced in fig. 1. It can be seen that the reflections are too much overlapped and the magnetic intensities too weak for very much to be deduced from them alone.

From the definition of the L vectors it can be seen that when $\mathbf{L}_2 = 0$

$$\mathbf{S}_1 = -\mathbf{S}_3 = \tfrac{1}{4}(\mathbf{L}_1 + \mathbf{L}_3),$$
$$\mathbf{S}_2 = -\mathbf{S}_4 = \tfrac{1}{4}(\mathbf{L}_3 - \mathbf{L}_1).$$

The spin vectors therefore lie in the (001) plane and the two spin directions are inclined at 71° ± 6° to one another. The total moment on each iron atom is $0{\cdot}73 \pm 0{\cdot}06\,\mu_B$.

§ 4. DETERMINATION OF THE NÉEL TEMPERATURE

To determine the Néel temperature the single crystal was mounted in a cryostat in such a way that its temperature could be measured by a

Table 1. Observed and calculated magnetic scattering

hkl	$\|F\|^2$(obs.)	$\|F\|^2$(calc.)†	$\|F\|^2$(calc.)‡
100	0·771	0·768	0·778
101	0·358	0·448	0·513
102	0·585	0·644	0·761
210	0·403	0·478	0·483
300	0·390	0·326	0·329
103	0·224	0·155	0·190
301	0·180	0·156	0·158
302	0·307	0·228	0·251

† $\mathbf{L}_1$ and $\mathbf{L}_3$ in orientations given by least squares analysis.
‡ $\mathbf{L}_1$ and $\mathbf{L}_3$ perpendicular to c.

Table 2. Observed and calculated nuclear scattering

hkl	$\|F\|^2$(obs.)	$\|F\|^2$(calc.)
Single crystal measurements		
002	6·51	7·39
202	13·12	39·0
204	2·19	2·03
004	29·3	108·1
402	18·7	74·8
200	1·98	2·03
400	1·13	0·88
Powder measurements		
110	2·97	2·94
200	2·00	2·03

Fig. 1

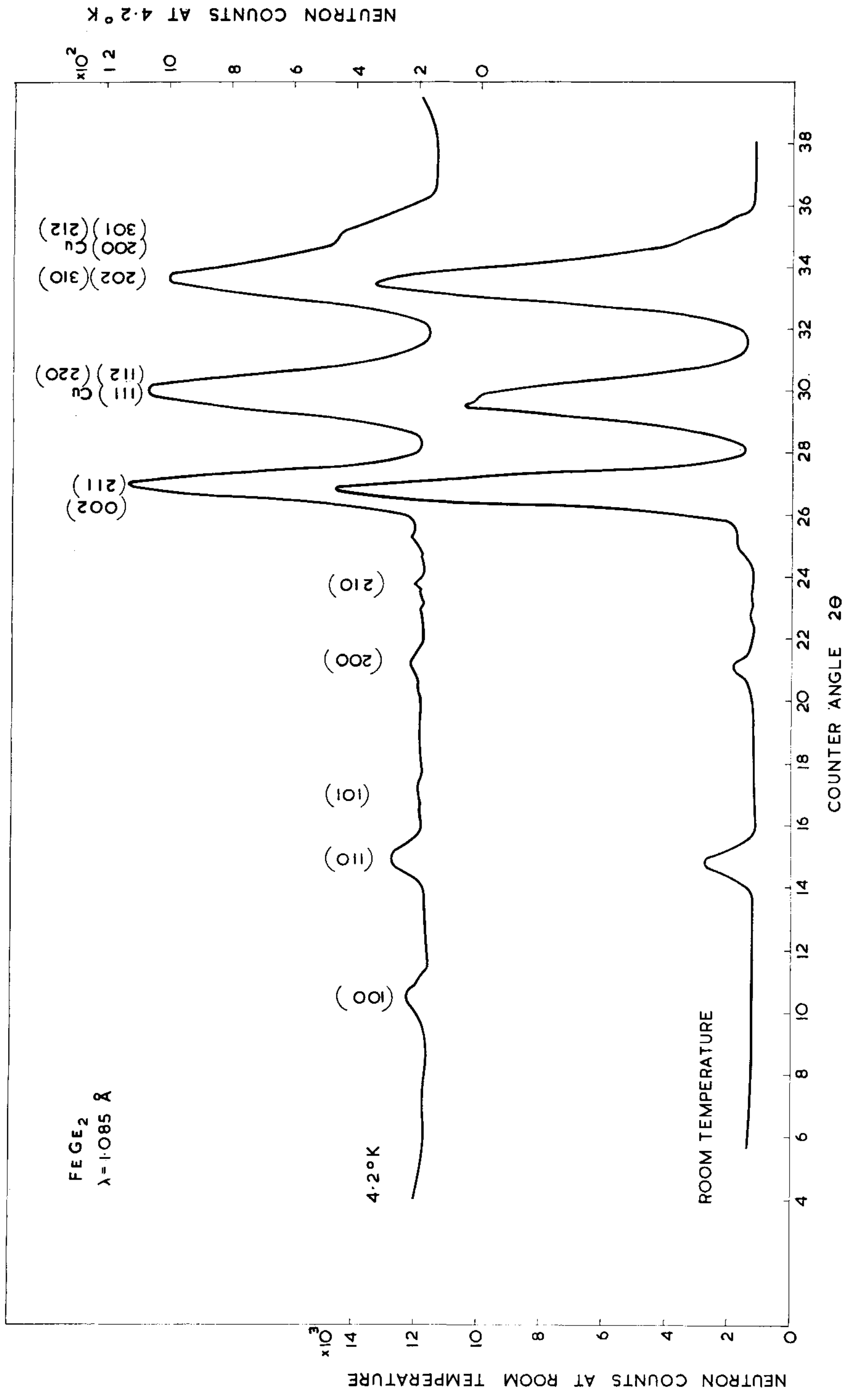

Powder neutron diffraction patterns of FeGe$_2$ at room temperature and 4·2°K.

thermocouple, one junction of which was in contact with the crystal. The crystal and counter were set so as to record the peak of the (100) magnetic reflection and the crystal was allowed to warm up slowly to room temperature from liquid nitrogen temperature. During this process simultaneous measurements of temperature and peak intensity were made. The results are shown in fig. 2; by extrapolating the steep part of the curve the Néel temperature is found to be about 270°K. The final tail of the curve is probably caused by short-range order.

Re-examination of the susceptibility measurements of Airoldi and Pauthenet shows a small but perceptible peak at about 270°K which is probably due to the anti-ferromagnetic transition.

§ 5. MÖSSBAUER EFFECT

Using a thin sample of $FeGe_2$ which had been crushed to a fine powder the Mössbauer effect of the Fe^{57} nuclei was studied with a single line source of Co^{57} in chromium. Measurements were made at 77°K and at a few temperatures between 0°C and room temperature (22°C); the data are summarized in table 3. From the disappearance of the hyperfine field, as the sample was warmed up, the Néel temperature was estimated to be 287 ± 2°K. This value is significantly different from that derived from the magnetic scattering measurements and it may be that the higher value obtained from the hyperfine field measurement is associated with the

Fig. 2

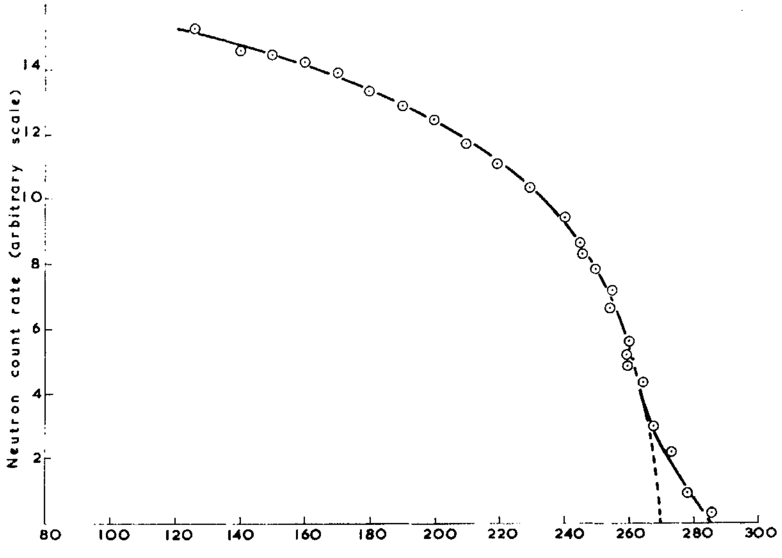

Variation of the peak intensity of the (100) magnetic reflection as a function of temperature.

existence of a considerable degree of short range order above 270°K as suggested by the 'tail' of the curve in fig. 2. It should perhaps be pointed out that the discrepancy is unlikely to be caused by errors in the thermocouple calibrations as both measurements were made with respect to the ice-point 273·2°K. Further work to clarify this point is planned.

The measured value of 148 kG for the hyperfine field at 77°K is consistent with the value for the moment derived from the neutron scattering although this value is rather lower than the value of 1 μB which would be predicted on the basis of a simple proportionality between atomic moment and hyperfine field. The positive value of the isomer shift indicates a decrease in s-electron density at the iron nucleus compared to that in pure iron. This could be associated with a decrease in the number of electrons in the conduction band (Walker *et al.* 1961) or with an increase in the number of 3d electrons giving increased screening and a magnetic moment less than that in pure iron. The measured electric field gradient q of table 3 is in the basal plane, along the direction of spin alignment. The field gradient along the tetragonal axis has twice this magnitude and is opposite in sign. This shows that the distortion of the charge distribution on the iron atoms is an elongation parallel to the tetragonal axis.

§ 6. DISCUSSION

The relative spin directions on the four iron atoms in the unit cell are shown in fig. 3 which is a projection of the structure on (001). Within layers parallel to (001) the coupling between atoms is purely anti-ferromagnetic but the spins in successive layers are inclined to one another at 71°.

An indication of the possible exchange paths may be obtained by reference to fig. 4. The iron–iron distances involved are $d_1 = 2{\cdot}48$ Å, $d_2 = 4{\cdot}18$ Å and $d_3 = 4{\cdot}86$ Å. The distance d_1 is closely similar to that in alpha iron and is therefore favourable for ferromagnetic coupling. The other two distances are too long for direct exchange and the magnetic coupling must involve their germanium neighbours. For all three iron–iron interactions exchange

Table 3

Temperature (°K)	Hyperfine field (kG)	Shift relative to iron at room temp. (mm/sec)	Quadrupole splitting $\frac{1}{2}e^2Qq$† (mm/sec)
77	148 ± 2	+0·47	+0·052
273	80 ± 4	+0·35	(1)
277	64 ± 2	+0·35	(1)
294	0	+0·35	~0·1 (2)

† In the expression for the quadrupole splitting, Q is the quadrupole moment and q the electric field gradient. (1) Magnetic and quadrupole splittings not resolved. (2) Estimated from the linewidth; splitting not resolved, q parallel to c.

Fig. 3

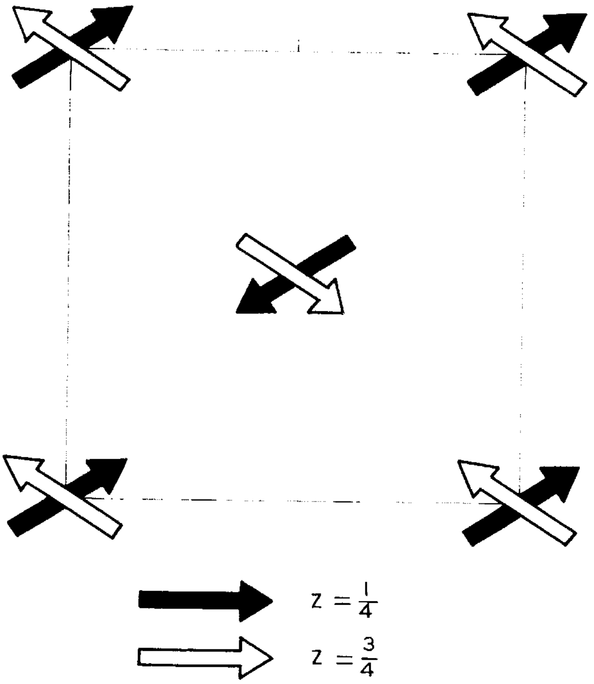

Relative orientations of the spin directions in $FeGe_2$ projected on (001).

Fig. 4

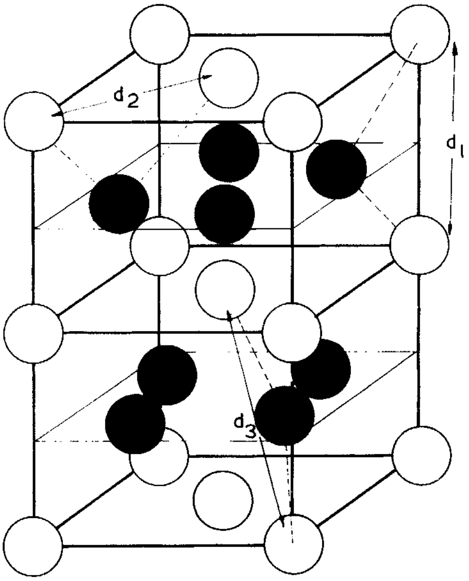

Schematic diagram of the structure of $FeGe_2$. The open circles represent iron atoms and the solid ones germanium atoms.

paths involving a single germanium atom exist. The lack of pure ferromagnetic coupling between the iron atoms distance d_1 apart may result from the existence of these two possible exchange mechanisms.

It should be noted that the non-collinear spin array in $FeGe_2$ cannot be attributed to non-isotropic exchange interactions of the type proposed by Dzialoshinskii (1958) and Moriya (1960) for α-Fe_2O_3, $MnCO_3$ and $CoCO_3$ and by Bertaut (1962 a, b) and Naish and Turov (1961) for $CoSO_4$ and the rare-earth orthoferrites. The vectors $\mathbf{L}_1$ and $\mathbf{L}_3$ defined previously transform according to different irreducible representations of the space group Imcm or of any sub-group which preserves the centres of symmetry at 000, $00\frac{1}{2}$, $\frac{1}{2}\frac{1}{2}0$, and $\frac{1}{2}\frac{1}{2}\frac{1}{2}$; whereas the condition given by the authors mentioned above for two magnetic modes to combine is that the vectors representing the directions of the spins on the sub-lattices for the two modes, in our case $\mathbf{L}_1$ and $\mathbf{L}_3$, should transform according to the same irreducible representation of the space group.

ACKNOWLEDGMENTS

We are grateful to Mr. J. H. Harrison for the provision of specimens and to Mr. L. Chaney, Mr. A. Cox and Mr. G. A. Briggs for experimental assistance. One of us (P. J. B.) wishes to thank the Solid State Physics Division, Harwell, for the opportunity to work there as a Vacation Associate.

REFERENCES

AIROLDI, G., and PAUTHENET, R., 1964, *C.R. Acad. Sci., Paris*, **258,** 3994.
BERTAUT, E. F., 1962 a, *J. Phys. Radium*, **23,** 460; 1962 b, *J. appl. Phys.*, Suppl., **33,** 1138.
DZIALOSHINSKII, I., 1958, *J. Phys. Chem. Solids*, **4,** 241.
FRAZER, B. C., and BROWN, P. J., 1962, *Phys. Rev.*, **125,** 1283.
MORIYA, T., 1960, *Phys. Rev.*, **120,** 91.
NAISH, V. YE., and TUROV, A. YE., 1961, *Fiz. Metal Metalloved*, **11,** 291.
PICKART, S. J., and NATHANS, R., 1961, *Phys. Rev.*, **123,** 1163.
WALKER, L. R., WERTHEIM, G. K., and JACCARINO, V., 1961, *Phys. Rev. Letters*, **6,** 98.
WALLBAUM, H. J., 1943, *Z. Metallk.*, **35,** 218.
YASHUKOCHI, K., KANEMATSU, K., and OHOYAMA, T., 1961, *J. Phys. Soc. Japan*, **16,** 429.